International Journal of Automotive Technology, Vol. 7, No. 4, pp. 449–457 (2006)

1229-9138/2006/028-08

DRIVER STEERING MODEL AND IMPROVEMENT TECHNIQUE OF VEHICLE MOVEMENT PERFORMANCE DURING DRIFT RUNNING

H. NOZAKI*

Department of Mechanical Engineering, Faculty of Science and Engineering, Kinki University, 3-4-1 Kowakae, Higashiosaka-shi 577-8502, Japan

(Received 20 December 2005; Revised 14 April 2006)

ABSTRACT–The driver model during drift cornering was examined, and a technique to improve vehicle movement performance during drift cornering was investigated. Based on the results obtained, the driver was found to steer using feedback of the body slip angle and the body slip angle velocity during drift cornering. Moreover, improvement of the cornering force characteristic, at which exceeded the maximum cornering force calm as much as possible is important.

KEY WORDS : Maneuverability, Human engineering, Automobile, Vehicle dynamics, Driver model, Drift control, Simulation

NOMENCLATURE

m : vehicle mass {1,500 kg}
I : yaw moment of inertia {240 kgm^2}
l : wheel base {2.62 m}
l_f, l_r : distance of front and rear axles from vehicle center of gravity {1.18, 1.44 m}
N : overall steering gear ratio {15.4}
δ_H : steering angle
δ_f : front wheel steering angle ($\delta_f = \delta_H/N$)
r : yaw rate
$\dot{r}$: yaw angle acceleration
β : vehicle body side-slip angle
β_f, β_r : side-slip angle of front and rear wheels
V : vehicle forward speed
F_f, F_r : cornering force of front and rear wheels
W_f, W_r : vertical load of front and rear wheels
$W_{f\text{-}in}$, $W_{f\text{-}out}$, $W_{r\text{-}in}$, $W_{r\text{-}out}$: vertical load of inside and outside wheels in cornering (front and rear wheels)
Δw_f, Δw_r : vertical load movement of inside and outside wheels in cornering (front and rear wheels)
μ : coefficient of friction of road
F_t : tire cornering force
β_t : tire slip angle
K_t : tire cornering power
y_{OL} : lateral displacement of target course
L : distance to eye point
ε : lateral displacement difference between eye point and target course
k : proportional constant

*Corresponding author. e-mail: nozaki@mech.kindai.ac.jp

1. INTRODUCTION

Drivers often perform counter steering in order to avoid accidents in regions that receive a great deal of snowfall. The direction of a vehicle can be changed through drift cornering even when the vehicle cannot be controlled using the steering wheel. Such emergency driving operations were investigated in a model by Amano *et al.* (1998; 1999) and Shimura *et al.* (2000). A driver model of counter steering during a spin was investigated by Sugasawa (2002). This paper was clarified the driver operation model during drift running. The present study investigates the ease of control in such a state of drift. In addition, a steering model for drift running was examined, and the improvement of the performance of the vehicle movement during drift running was examined using the model.

2. DESCRIPTION OF VEHICLE MOVEMENT

2.1. Equation of Motion

An analysis of the movement of the vehicle was performed using a vehicle model with two degrees of freedom (Figure 1).

The equation of motion is as follows:

$$mV(\dot{\beta}+r)=F_f+F_r \tag{1}$$

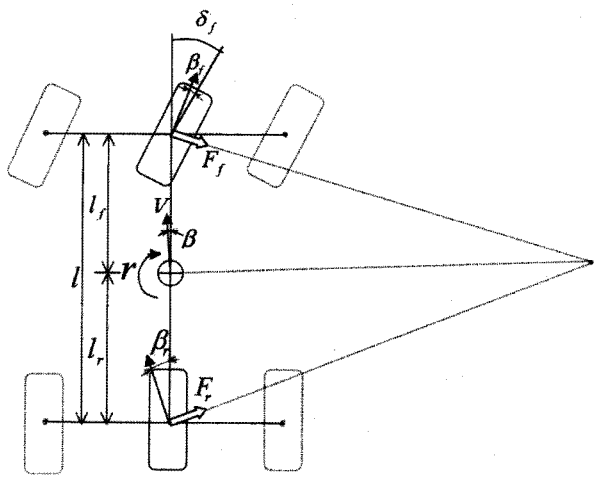

Figure 1. Vehicle model (bicycle model).

$$I\dot{r} = l_f F_f - l_r F_r \tag{2}$$

Moreover, in order to simplify the analysis, the tire slip angles of the right and left wheels are assumed to be equal, so that the front and rear wheel slip angles are as follows:

$$\beta_f = \delta_f - \beta - l_f r/V \tag{3}$$

$$\beta_r = -\beta + l_f\, r/V \tag{4}$$

The normal loads on the tires of right and left wheels, which are considered to be the loads associated with lateral acceleration, are given below:

$$\left.\begin{aligned} W_{f-in} &= W_f/2 - \Delta w_f \\ W_{f-out} &= W_f/2 + \Delta w_f \\ W_{r-in} &= W_r/2 - \Delta w_r \\ W_{r-out} &= W_r/2 + \Delta w_r \end{aligned}\right\} \tag{5}$$

The cornering force characteristics of the front and rear wheels are obtained as a function of the slip angle and the vertical load of the tires of the front and rear wheels. The cornering force characteristics of the tires is based on an equation reported by Fiala (1954). The two cases shown in Figure 2 are used for cases in which the maximum cornering force is exceeded.

$$\left.\begin{aligned} &F_t = f(\varphi)(\mu W) \\ &\text{where:} \\ &f(\varphi) = \varphi - |\varphi|\varphi/3 + \varphi^3/27 \quad (|\varphi| \le 3) \\ &\varphi = K_t \tan\beta_t/\mu W \end{aligned}\right\} \tag{6}$$

When φ is 3 or greater, two tire cases are obtained (Figure 2).

In Tire Case A, the equation is as follows:

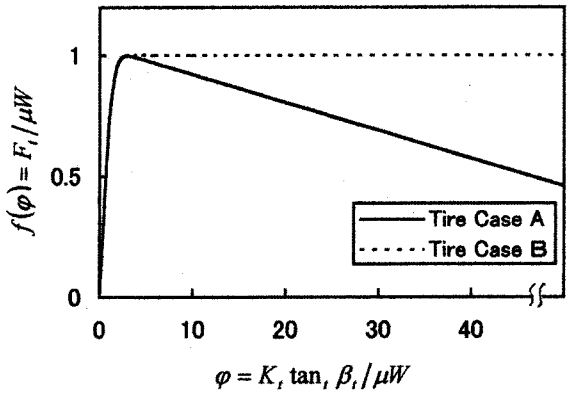

Figure 2. Tire model.

$$f(\varphi) = 1 - 1/87(|\varphi| - 3) \quad (|\varphi| > 3)$$

That is, the maximum value was exceeded, and a decreasing characteristic is assumed. In Tire Case B, the equation is as follows:

$$f(\varphi) = 1 \quad (|\varphi| > 3)$$

Here, μ of the rear wheels was set lower than that of the front wheels in order to allow ease of drifting.

2.2. Steering Model for Drift Cornering

The eye point of a driver during drift cornering was recorded using an eye camera. The eye point of the driver is related to the body slip angle as shown in Figure 3. The driver perceives the progress direction vector of the body, and controls the counter steering angle so as to maintain the drift angle. Accordingly, in the driver steering model for drift cornering, the vehicle body slip angle and the vehicle body slip angle velocity were used as feedback.

The steering model for drift running to maintain an intentional drift angle in cornering was examined. The step steering angle upon cornering is as follows:

$$\delta_f = k_0 \mathrm{step}(t) \quad (|\beta| \le 10) \tag{7}$$

$$(\delta_H = N\delta_f)$$

(The steering angle is set such that the vehicle body slip angle β does not exceed 10 degrees.)

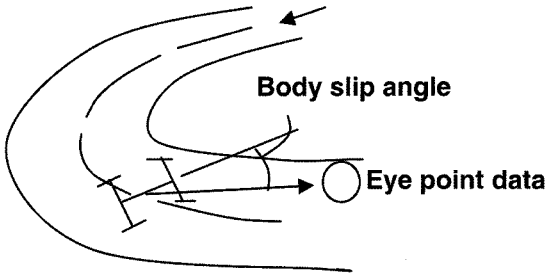

Figure 3. Eye point of driver during drift cornering.

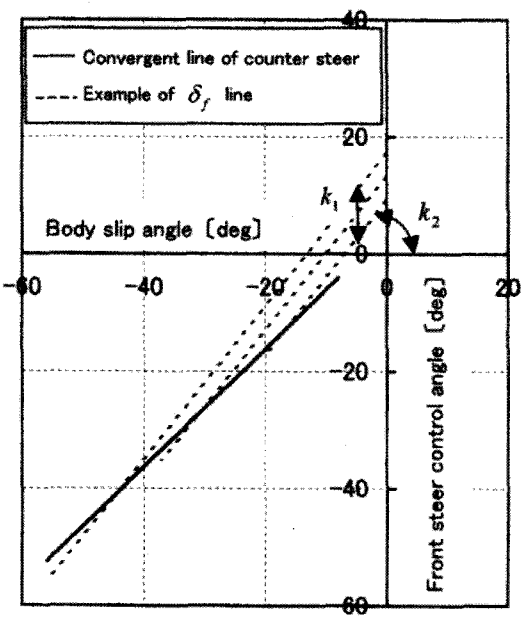

Figure 4. Counter steering model.

Next, the steering angle from the point in time when the vehicle body slip angle β exceeds 10 degrees was assumed to be as explained below. This indicates the control steering angle by which the drift angle in the drift region was maintained. That is, the steering model of the driver was assumed to be a model in which the vehicle body slip angle and vehicle body slip angle velocity were feedback.

$$\delta_f=(k_1+\beta)\times k_2+\dot{\beta}\times k_3 \quad (|\beta|>10) \tag{8}$$

$$(\delta_H=N\delta_f)$$

The drift control steering angle of Equation (8) is shown in Figure 4.

The inclination of the control steering angle changes when k_2 is changed, as shown by the dotted line in Figure 4.

The dotted line shifts up or down when k_1 is changed. The solid line in Figure 4 indicates the relationship between the vehicle body slip angle and the front wheel steering angle when the front and rear wheels are balanced by counter steering during cornering. Therefore, if the steering angle intersects the solid line periodically and finally settles along a dotted line showing a drift control steering angle, indicating balance, the drift angle can be maintained during turning.

In addition, since a delay in feedback steering was caused when steering was proportionate to the vehicle body slip angle β, the forecast feedback steering by coefficient k_3 at the vehicle body slip angle velocity $\dot{\beta}$ was added as a differentiation element.

3. DRIFT CORNERING SIMULATION RESULT

3.1. Influence of Decrease in Cornering Force When the Maximum Cornering Force of Tire is Exceeded

The improvement of the performance of the vehicle movement during drift running was examined by a simulation analysis.

Figure 5 shows the trajectory upon drift cornering for two types of tires. Figure 6 shows the trajectory of Tire A. Step steering of 100 deg was performed for approximately one second, after which counter steering was performed. It is understood not to settle to the target drift angle. The body slip angle, turn lateral acceleration, and yaw rate of the vehicle are shown in the figure.

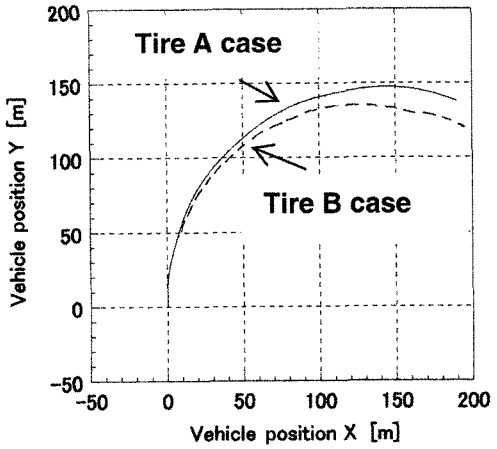

Figure 5. Running trajectory.

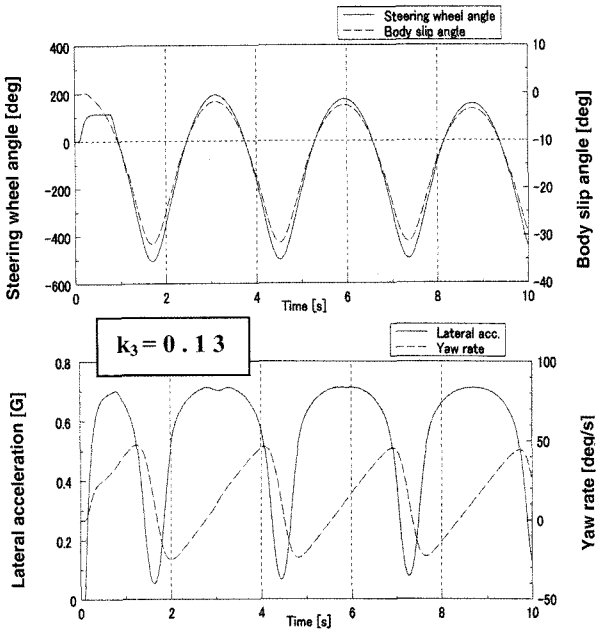

Figure 6. Simulation results (tire A case).

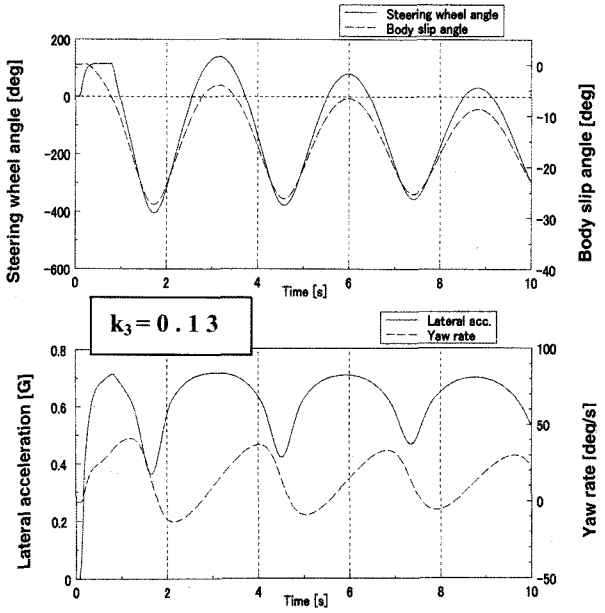

Figure 7. Simulation results (tire B case).

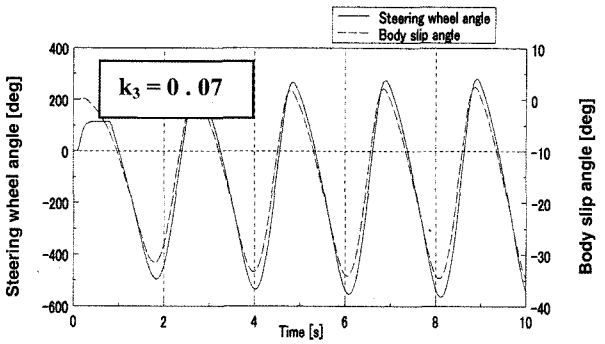

Figure 8. Simulation results (tire B case).

On the other hand, the control steering angle required to maintain the drift angle in the case of Tire B is shown in Figure 7 and has a tendency to settle.

Similarly, Figure 8 shows the results for a body slip angle velocity coefficient k_3 of approximately half that of for the case of Tire B. As a result, the drift control shows repeated vibration, as in the case of Tire A.

That is, as the characteristic of the tire approaches that of Tire B, the slip behavior of the vehicle is achieved at slower speeds. As a result, the driver can perform drift control with considerable ease. Here, calculation is performed with k_1=10, k_2=1.5.

3.2. Influence of constants k_1, k_2 and k_3 on the simulation equation of drift control steering angle

The drift angle changes when constant k_1 of the target drift angle in the constant of the feedback steering is changed (Figure 9).

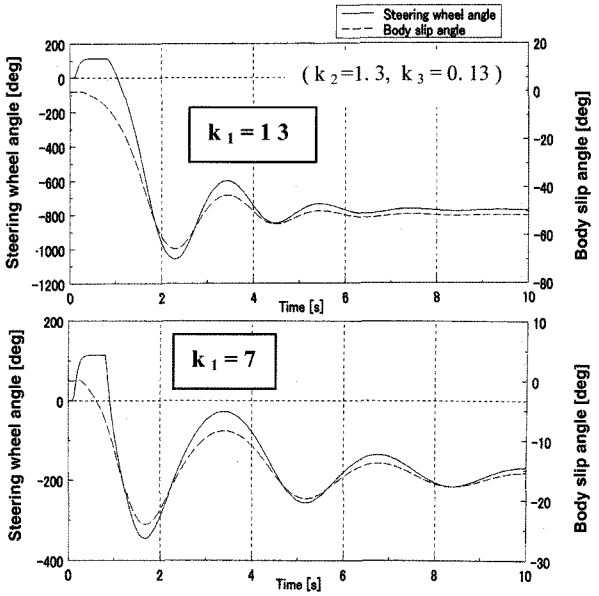

Figure 9. Simulation results (effect of k_1).

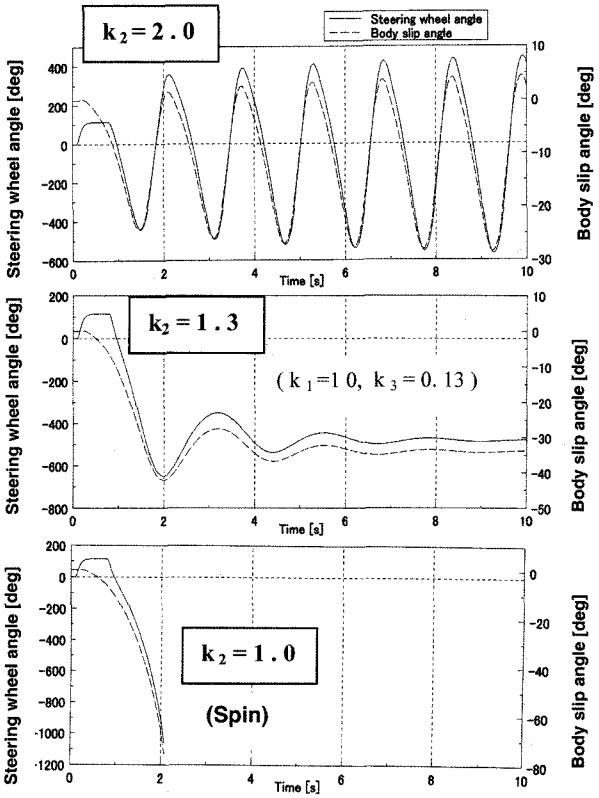

Figure 10. Simulation results (effect of k_2).

In addition, the appearance of settling changes when constant k_2 of the vehicle body slip angle changes, and the vehicle entered a spin when counter steering was insufficient (Figure 10).

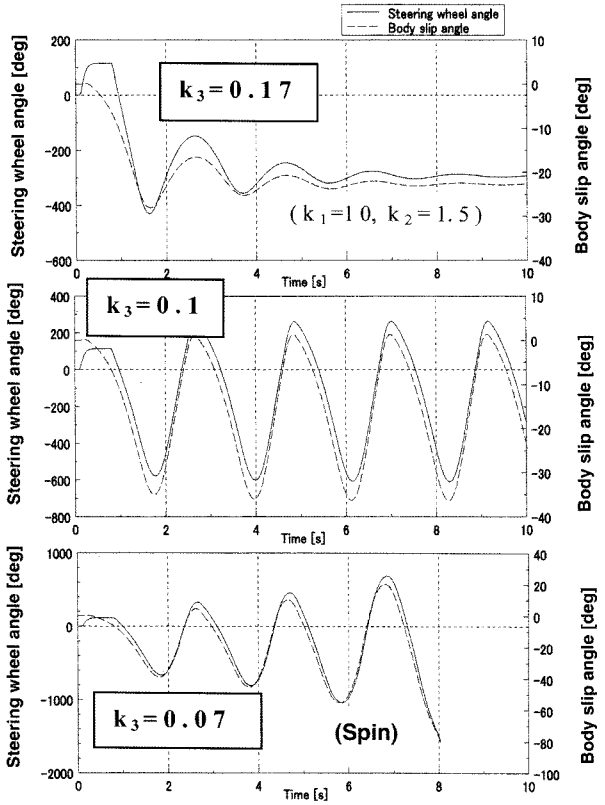

Figure 11. Simulation results (effect of k_3).

When constant k_3 of the vehicle body slip angle velocity changed, the target drift angle was easily reached because the phase of the steering angle advanced (Figure 11).

Therefore, the drift angle in the direction of settling can be achieved by controlling the drift angle according to the value of coefficient k_1 of the vehicle body slip angle and assuming the value of k_2 to be a moderate inclination in the driver model.

In addition, settling at the drift angle is easily achieved by enlarging the value of coefficient k_3 at some vehicle body slip angle velocity, which is the differentiation element, to be small.

4. EXPERIMENTAL RESULTS BY DRIVING SIMULATOR

4.1. Outline of Experiment Device (Driving Simulator)

A running experiment was performed using a driving simulator (Virtual Mechanics Company), as shown in Figure 12. Regarding the simulator, a visual display and sound generation system simulating the engine sound of a vehicle when running were built in to reproduce an actual driving situation. In the experiments, the following items were measured.

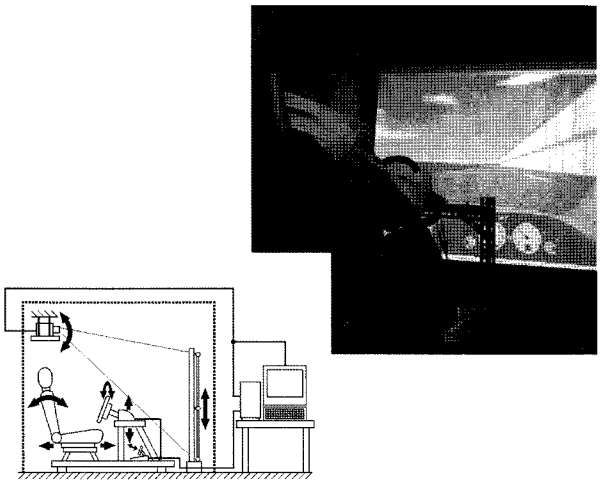

Figure 12. Driving simulator.

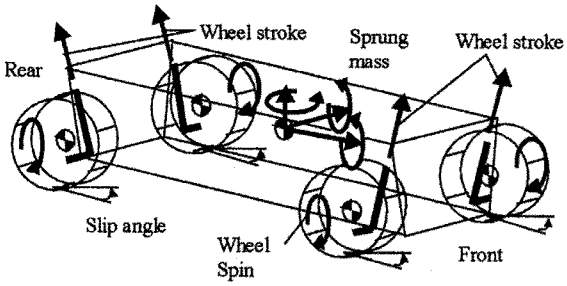

Figure 13. Primary components and degrees of freedom of the vehicle model.

Vehicle drive state data: steer angle, steer torque, vehicle velocity, positional data, body slip angle, yaw rate, yaw angle, roll angle, pitch angle, lateral acceleration, and the steer angle of each wheel, etc.

4.2. Vehicle Model and Vehicle Characteristics

As a vehicle model, the driving simulator uses the full vehicle movement simulation software named CarSim (Version 5.16) of the mechanical simulation corporation (MSC Co., USA). Figure 13 shows a schematic diagram of the vehicle model. Table 1 shows a number of the primary components of the vehicle and indicates the degrees of freedom. For example, the rear axle is rigid

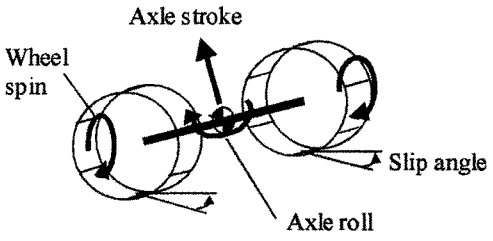

Figure 14. Solid-axle movement.

Table 1. Components and degrees of freedom of the vehicle model.

Bodies	
Sprung mass body	1
Unsprung mass bodies (wheel carriers)	4
Rotating wheels	4
Engine crankshaft	1
Total	10
Degrees of freedom	
Sprung body translation (X, Y, Z)	3
Sprung body rotation (yaw, pitch, roll)	3
Suspension stroke	4
Wheel spin	4
Powertrain (Engine crank shaft)	1
Tire delayed slip (lateral, longitudinal)	8
Brake fluid pressure	4
Total	27

Table 2. Specifications of vehicle.

Width of vehicle (mm)	1500
Wheelbase (mm)	2690
Distance from center of front axle to rear end of vehicle (mm)	3800
Distance from center of front axle to center of gravity (mm)	1014
Height from ground to center of gravity (mm)	542
Vehicle mass (kg)	527
Roll moment of inertia (kg·m^2)	606.1
Pitch moment of inertia (kg·m^2)	2741.9
Yaw moment of inertia (kg·m^2)	2741.9

and has two freedom degrees: vertical movement and rotation of the axle (Figure 14). Details are provided in Reference (Watanabe *et al.*, 2002).

The vehicle model has an FR layout (front-mounted engine, rear-wheel drive), which is particularly susceptible to drift. Table 2 shows the specifications of the parameters of the vehicle model used in the experiment.

The tire cornering force characteristic used for the experiment is the two tire characteristic, as shown in Figure 15.

In addition, the tire characteristic during driving and braking is assumed to be as shown in Figure 16. By adding the slip angle and the slip ratio for a specific time, the concept of the friction circle based on the calculation of the combined characteristic of CarSim is applied. Therefore, the vehicle tends to enter spins because the lateral force of the rear wheel decreases when accelerating during critical cornering. Thus, drift cornering can be achieved by counter steering, and a real car running under conditions in which the maximum cornering force is exceeded can be simulated.

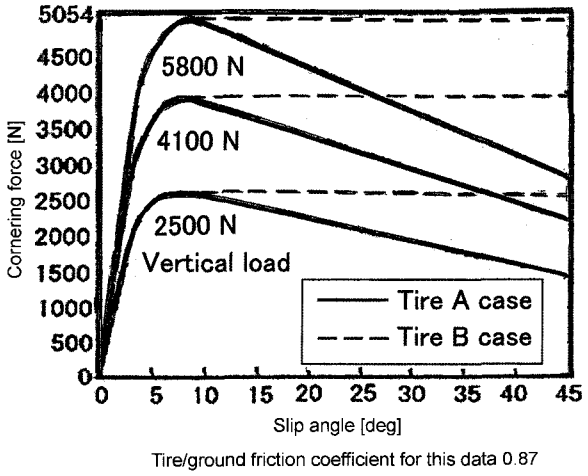

Figure 15. Tire cornering force characteristic.

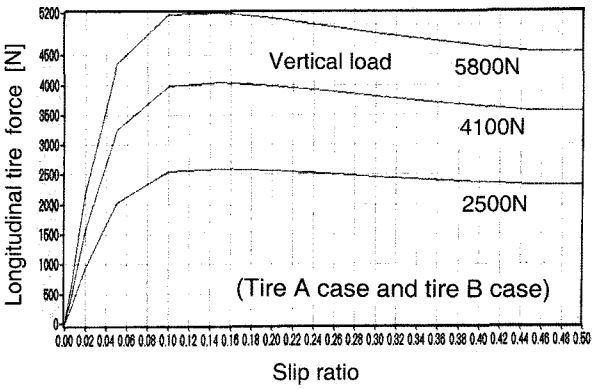

Figure 16. Longitudinal tire force characteristic.

4.3. Experimental Results

Figures 17 and 18 show the obtained results. In this experiment, the vehicle is accelerated to a high lateral acceleration during a 75-m-radius turn, inducing intentional sliding of the rear wheels, and the driver applies counter steering. The driver controls the counter steering angle to maintain a drift turn of 75 m in radius while maintaining the drift angle (Figure 17). In addition, the driver intentionally engaged the accelerator, generating a power slide, upon which time the driver released the accelerator slightly, so that this state was maintained as long as possible. As a result, the vehicle velocity of the drift cornering was maintained within the range of 85–95 km/h. That is, counter steering became the primary means of drift control under these experiment conditions. The driver was somewhat accustomed to drift control in

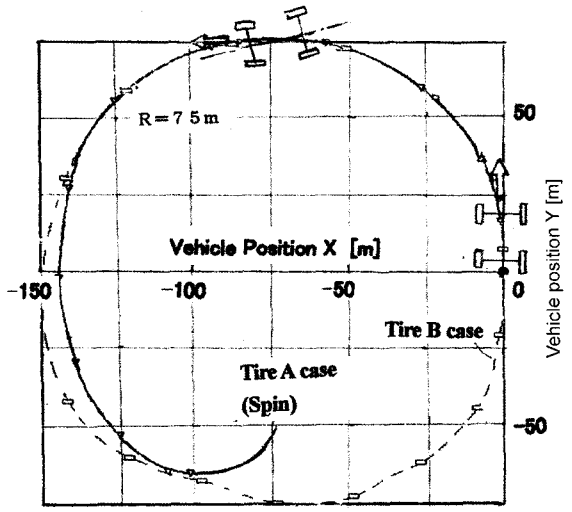

Figure 17. Experimental results for running trajectory obtained using the driving simulator.

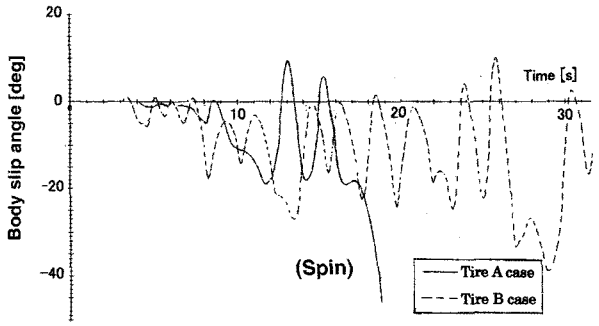

Figure 18. Experimental results for body slip angle obtained using the driving simulator.

the driving simulator. As a result, maintaining the drift angle through spin became difficult in the Tire A case, in which the cornering force decreases after having exceeded the maximum cornering force while turning. On the other hand, the drift angle was maintained and the drift control was far easier in the Tire B case, in which the cornering force was assumed to be constant after having exceeded the maximum cornering force. Figure 17 shows the running trajectory of the drift turn. Figure 18 shows the change in the body slip angle with elapsed time. In the Tire A case, the driving is emanated vibrating. On the other hand, in the Tire B case, the drift angle was maintained during counter steering and the return of the counter steering.

5. TEST VEHICLE RUNNING TEST RESULTS

The vehicle test was performed on a test course of a skidpad of 40 m in radius. The driver slides the rear wheel by engaging the accelerator during high-lateral-acceleration cornering. The vehicle velocity for the drift cornering is approximately 60 km/h. In addition, the driver controls the counter steering angle and maintains the semicircle drift angles to a certain degree. The driver was somewhat accustomed to drift control in the driving simulator and performed the test 10 times. Two types of tires were used in this test. Tire a case is a standard radial tire, and Tire b case is a racing-type tire with a low decrease in cornering force after the maximum cornering force has been exceeded. In contrast with Tire a case, it was possible to control the vehicle without spinning during drift running for Tire b case (Table 3). That is, the stability was greatly improved. The drift was easily controlled in the running test for tires in which the decrease in cornering force was suppressed, where the maximum cornering force of the tire had been exceeded.

Table 3. Experimental results by test vehicle (average value).

Tire	Generation ratio of spin at the drift control (%)
Tire a case	0 [%]
Tire b case	50 [%]

6. ADDITIONAL EXPERIMENTAL SIMULATION OF A SEVERE LANE CHANGE WITH DRIFT

6.1. Steering Model for Lane Change with Drift

The steering model of the driver assumed that the driver to be looking in the forward direction of the vehicle L[m]. In addition, the deflection ε between the lateral displacement of the vehicle which will be caused in the becoming time of L/V when advancing L[m] like present posture and the target course is detected and used for feedback control (Figure 19).

That is, it is assumed that the eye point model is

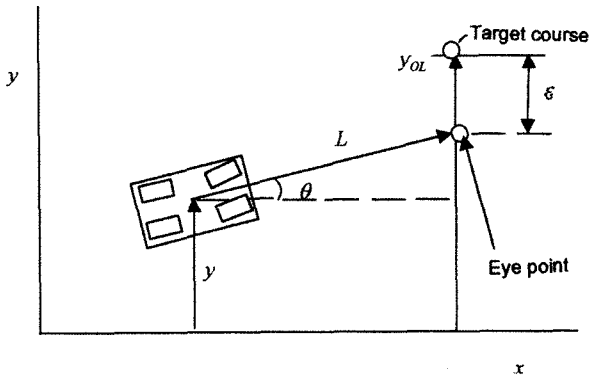

Figure 19. Driver steering model (lane change with drift).

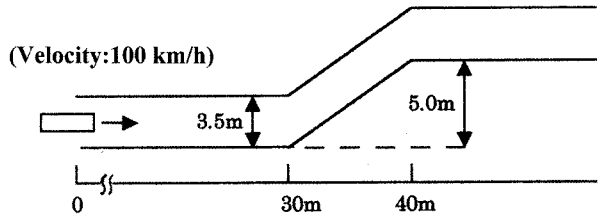

Figure 20. Lane change course.

looking forward. The deflection ε between the eye point and the target course is as follows:

$$\varepsilon = y + L\sin\theta - y_{OL} \tag{9}$$

$$\delta_H = N \times (k \times \varepsilon) \tag{10}$$

where L was assumed to be 14 m and k was assumed to be -1.5.

6.2. Drift Running Simulation Result

In the following, an emergency lane change is simulated, as shown in Figure 20 (Vehicle velocity: 100 km/h).

6.3. Influence of Decrease in Cornering Force in Area at which the Maximum Cornering Force of the Tire is Exceeded

The influence of the difference in tire characteristics for two types of tire was simulated. The influence of difference in area at which the maximum cornering force of the tire was exceeded was investigated. Figure 21 shows simulation results for a severe lane change for the case of Tire A, in which the steering angle was approximately 200 deg for approximately 1 second from the start of cornering. Counter steering was applied afterwards because the rear wheels skid, and the vehicle posture is controlled. In addition, the body slip angle, lateral acceleration and the state of lateral displacement are shown. Approximately 3.5 seconds after cornering, a transient overshoot of lateral displacement of the vehicle of approximately 2 m occurs. In addition, after approximately 6 seconds, the vehicle settled into the target lane at lateral displacement of 5 m. Counter steering was found to be approximately proportional to the body slip angle. Figure 22 shows the simulation results for a severe lane change for the Tire B case. Approximately 3 seconds after cornering, a transient overshoot of lateral displacement of the body of approximately 1.5 m is caused. The vehicle settled into the target lane at lateral displacement of 5 m approximately four seconds later. Moreover, the counter steering was found to be approximately proportional to the body slip angle, as in the Tire A case. That is, upon a severe lane change with drift, the transient overshoot of lateral displacement of the vehicle was decreased when the cornering force became smooth in the area where the maximum cornering force was exceeded. Settling was also greatly improved.

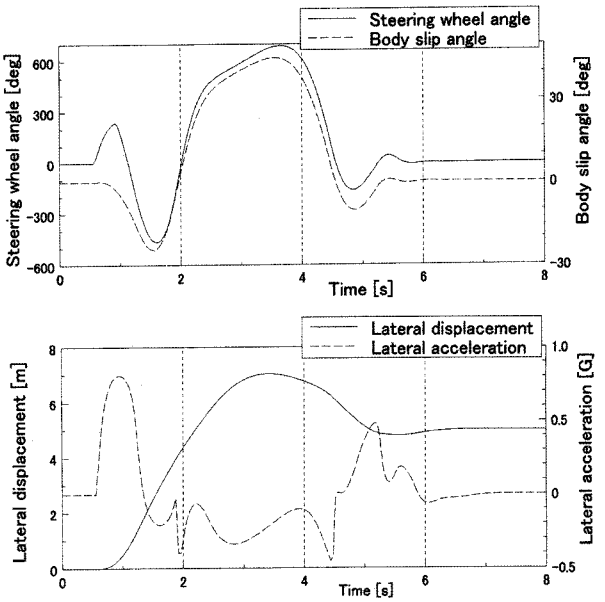

Figure 21. Simulation results of drift running (tire A case).

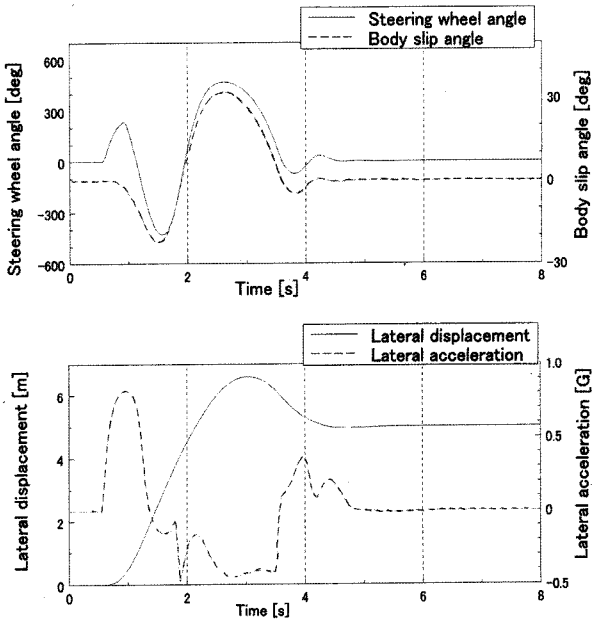

Figure 22. Simulation results of drift running (tire B case).

7. CONCLUSIONS

(1) The use of tires that decrease to the greatest extent possible the cornering force of the area where the tire cornering force of the rear wheels exceeds the maximum cornering force is an effective technique

by which to improve drift control. The slip behavior of a vehicle having such tires becomes smooth and the drift control becomes much easier.

(2) When the drift was controlled, the driver was able to judge the feedback of primarily the body slip angle to decide the necessary counter steering angle in order to maintain the target drift angle. In addition, because feedback steering was accompanied by some delays, the body slip angle velocity was also used for feedback steering in order to provide differential steering by which the phase was advanced.

In the present study, the mechanism of drift control was examined. Future studies will examine various additional considerations. In addition, in order to improve the movement performance of the vehicle, a new steering wheel control system will be examined.

REFERENCES

Amano, Y., Hada, M., and Doi, S. (1998). A model of driver's behavior in ordinary and emergent situations. *TOYOTA Laboratory R&D Review* **33, 1**, 23–30 (in Japanese).

Amano, Y., Nagiri, S., Hada, Y. and Doi, S. (1999). A driver behavior model in emergency situations. *Trans. Japan Society of Mechanical Engineers (JSME J.)*, **65-632, C**, 282–288 (in Japanese).

Fiala, E. (1954). Seitenkrafte am rollenden luftreifen. *Verein Deutscher Ingenieure (V.D.I.)*, **Bd.96, Nr.29, 11**.

Shimura, A. and Yoshida, K. (2000). Acquisition of car cornering operation by means of neural networks and genetic algorithms. *Trans. Japan Society of Mechanical Engineers (JSME J.)*, **66-642, C**, 232–237, (in Japanese).

Sugasawa, F. (2002). Study on driver model for counter steer at vehicle spinning. *Proc. Society of Automotive Engineers of Japan, Inc. (JSAE) Annual Congress*, **6-02**, 7–10 (in Japanese).

Watanabe, Y., Michael, W. Sayers. (2002). Extending vehicle dynamics software for analysis, design, control, and real-time testing. *Proc. AVEC'02*, **20024545**, 407–412.